Clays and Clay Minerals, Vol. 58, No. 2, 220–237, 2010.

FACTORS INFLUENCING THE FORMATION AND CHARACTERISTICS OF HALLOYSITES OR KAOLINITES IN GRANITIC AND TUFFACEOUS SAPROLITES IN HONG KONG

GORDON JOCK CHURCHMAN[1,2,*], IAN RUSSELL PONTIFEX[3], AND STUART GERRAND MCCLURE[1,2]

[1] CSIRO Land and Water, Glen Osmond, South Australia 5064
[2] School of Earth and Environmental Sciences, University of Adelaide, South Australia 5005
[3] Pontifex and Associates, Kent Town, South Australia

Abstract—The occurrence of halloysite and/or kaolinite in clay-rich, vein-like zones in saprolites in Hong Kong has provided the opportunity to examine the conditions determining the formation of one kaolin mineral or the other and also the nature of their particles. Clay-rich zones within tuffaceous or granitic saprolites from six different hillside sites have been examined in replicate samples by optical and scanning electron microscopy, X-ray diffraction, and thermal analysis. Kaolin minerals, sometimes together with Mn oxides and Fe oxides/oxyhydroxides, have formed within discontinuities within the altered host rocks. The fabrics of kaolin infills generally indicated several generations of kaolin formation and that shear and deformation have commonly occurred within the infills. The infills were either light or dark in color. Light-colored infills often comprised pure, or nearly pure, halloysite or kaolinite. Dark Mn- and Fe-rich infills all contained kaolinite, while including some halloysite. The very halloysitic, light-colored infills occurred in saprolites in both granite and tuff as long tubular shapes in parallel bunches. The light-colored, very kaolinitic infills occurred in tuff only, in large platy or near-platy shapes within vermiform packets. In dark-colored infills, early kaolin mineral crystallization was limited by impurities from the breakdown of primary minerals leaving dissolved and re-precipitated compounds of Mn and Fe within the infill. Kaolin minerals in infill at all the sites except one are considered to have formed as a result of weathering. The exception comprises white infills in tuff that are composed of extremely small, closely packed particles, suggesting formation by hydrothermal action. Generally, the kaolin minerals have formed by neogenesis out of solution in the discontinuities. Drying, with the formation of Mn and/or Fe oxides/oxyhydroxides, had occurred several times, indicating enhanced drainage. Where drying had occurred, kaolinite had formed. Where indications of drying in infills were absent, halloysite was predominant.

Key Words—Fe Oxides/Oxyhydroxides, Infills, Mn Oxides, Rock Deformation, Shearing, Todorokite, Weathering.

INTRODUCTION

Halloysites and kaolinites have virtually identical chemical compositions, being composed of aluminosilicate layers comprising $Al_2Si_2O_5(OH)_4$, albeit with variations over a small range, except that a halloysite may have as many as two molecules of H_2O, as interlayer water, for each $Al_2Si_2O_5(OH)_4$. The fact that halloysite contains or formerly contained this additional water in its interlayers, prior to its loss by dehydration, has a decisive influence upon its crystal morphology, which is generally curled rather than platy like kaolinite (*e.g.* Bates *et al.*, 1950; Bailey, 1990; Singh, 1996; Joussein *et al.*, 2005). Halloysites are defined by the presence, or history, of interlayer water in a mineral with a kaolin layer structure (Churchman and Carr, 1975). However, chemical, structural, or crystallographic explanations for why halloysites contain water in their interlayers remain unconvincing, in spite of Bailey's (1990) hypothesis that a more negative charge in halloysite aluminosilicate layers than in those of kaolinites, which arises from a greater ^{IV}Al content, leads to charge compensation in the interlayers by hydrated cations. Subsequent analyses using nuclear magnetic resonance showed a range of halloysites to have only small ^{IV}Al contents and which were no greater than those of a range of kaolinites (Newman *et al.*, 1994), while Quasi-Elastic Neutron Scattering showed differences between the mobility of interlayer water in halloysite from that in montmorillonite that are consistent with the absence of cations from the interlayers of halloysite, whereas they occur, and influence water mobility, in montmorillonite interlayers (Bordallo *et al.*, 2008).

A project that aimed to help explain the role played by kaolin clay-rich vein-like zones within saprolites on slopes in Hong Kong in causing, or exacerbating, landslides there (*e.g.* Kirk *et al.*, 1997; Campbell *et al.*, 1998) focused on the detailed mineralogy of these zones as a basis for explaining relative slope stabilities. Both halloysite and kaolinite occurred in the kaolin clay-rich zones that were implicated as unstable areas of the

* E-mail address of corresponding author:
jock.churchman@adelaide.edu.au
DOI: 10.1346/CCMN.2010.0580207

landslide-prone slopes (Campbell *et al.*, 1998). The opportunity offered by this project to determine the conditions under which halloysite and kaolinite occurred either separately or together, and of the effect of different geological and environmental factors upon their particular occurrences and their characteristics, has enabled a search for generalizations about factors which influence the formation of halloysites or kaolinites and which give rise to many of their important features. The opportunity is available because some of the possible influences determining the particular kaolin mineral that had formed, such as rainfall and temperature, could be eliminated from consideration since the different kaolin clay-rich zones were found close together within the compact territory of Hong Kong. Nonetheless, the saprolites under consideration in the project were formed from either of two rock types, *i.e.* granite or volcanic tuff. The work described here focused on samples of saprolites taken from hill slopes because they incorporated clay-rich veins which were suspected to provide weak points in the landscape for the initiation of landslides. No attempt was made to select samples that were representative of the area or its geology.

MATERIALS AND METHODS

The main rock types constituting slopes in and adjoining the urban areas of Hong Kong are the granites and granodiorites of Upper Jurassic to Cretaceous age and an associated suite of volcanic rocks that is slightly older and which consists mostly of fine and coarse ash tuffs and rhyolites (Irfan, 1998). The granites and volcanic rocks are affected by faulting dating back to the Mesozoic (Irfan, 1998). Weathering has led to profiles that are characterized by four main zones, following Irfan (1998), *i.e.* (1) residual soil, (2) saprolite, (3) partially weathered rock, and (4) unweathered rock. The saprolite may be >60 m thick in granites and >20 m thick in volcanic rock, while the residual soil cover is generally thin or missing in many weathering profiles according to Irfan (1998). In the present study, saprolites on either granite or volcanic tuff were sampled for study. Nineteen different samples of saprolites from six separate hillside sites in Hong Kong were studied. All came from sites within a 15 km radius centered on the city of Kowloon (see, *e.g.* Irfan, 1996, 1998, for a geological map of Hong Kong). One site (from Shum Wan Road) was on Hong Kong Island; the remaining five were on the mainland. The primary interest was in kaolin-rich infill veins in the saprolites. The sampling locations, sample abbreviations, rock types, and field descriptions of the kaolin-rich infill veins are given in Table 1.

In each case, a sample was removed in a wet condition from the saprolite as a block ~100 mm × 100 mm × 50 mm in size which was enclosed in waxed paper and aluminum foil for air transport from Hong Kong to Australia so that it was still moist and intact when received and unwrapped.

Upon receipt, each of the samples was photographed and was then sub-sampled for mineralogical analyses, with small (generally <1 g) sub-samples being taken intact, using a scalpel, mainly from vein infill material, for this type of analysis. Part of the sub-sample was examined by scanning electron microscopy (SEM) using a Cambridge Stereoscan SEM S250 fitted with a Link energy-dispersive X-ray (EDX) detector. For this purpose, pieces of the intact material were dried at 105ºC and then mounted, maintaining their orientation from the original block sample so as to be able to relate results back to their field settings, and were coated with gold for morphological analyses or with carbon for elemental analyses (by EDX). Another part of each sub-sample, from the same location on the block as that taken for SEM, was used for X-ray diffraction (XRD) and also differential thermal (DTA) and thermogravimetric (TGA) analyses.

Material from the sub-samples for XRD analyses was in two different forms. Some was prepared as powdered whole samples by air-drying, followed by a light grinding. Approximately 90 mg was then analyzed as an unoriented powder in an aluminum sample holder, using a Philips 1800 X-ray diffractometer with CoKα radiation. The concentration of quartz in each sample was obtained by comparing the height of the strongest peak for quartz in the sample with that of the same peak in a quartz standard ('Arkansas stone,' supplied by Philips) that was analyzed soon before or afterwards. Carter *et al*. (1987) used Arkansas stone as an external standard for the analysis of the quartz content of bentonite samples. Another portion of the sub-sample was first separated into one or more particle-size fractions prior to their XRD analyses as oriented sediments. For this purpose, a sample that had been kept moist was dispersed in ~2% sodium hexametaphosphate in 0.025 M NaOH, using a mechanical mixer mill, and was sedimented and centrifuged for the appropriate time, following Stokes Law of settling (*e.g.* Jackson, 1956) in order to obtain the <2 μm fraction. This clay fraction material was settled out of suspension by adding 2 M $CaCl_2$ drop-wise to achieve flocculation and was washed free of salts using ethanol, after which it was air-dried. The clay fraction was analyzed by XRD after (1) re-dispersion in de-ionized water using an ultrasonic probe, (2) sedimentation onto porous ceramic tiles, (3) immediately following the addition of one or two drops of formamide (following Churchman *et al.*, 1984), and (4) heating the formamide-treated sample on the tile at 105ºC for 16 h and then at least 1 h after adding one or two drops of glycerol. X-ray diffraction, following formamide addition (3, above), enabled the relative proportions of kaolinite and halloysite, which made up the total kaolin mineral content, to be determined

Table 1. Sampling locations, sample abbreviations, rock types, and field descriptions (textures in bold) of the kaolin-rich infill veins.

Sample location	Sample names	Rock type	Field description of kaolin-rich infill veins*
Tiu Keng Leng	TKL 1 2 3 SP2E (East) SP2W (West)	Coarse-grained greisenized granite	Laterally persistent (>10 m) veins within discontinuities in completely decomposed granite; dip out of slope at 19−34°; maximum thickness of 50 mm; generally sub-parallel; sharp contact with saprolite; either soft to firm, reddish-yellow **silty clay** (TKL 1 and 3) or a very soft pale pink mottled white **clay** (TKL 2 and SP2E, W).
Sha Tin College	STC S1A S1OppC	Coarse-grained greisenized granite	Maximum thickness of 30 mm; often very diffuse contact with saprolite; slickensides common, black **sandy silt**.
Shek Kip Mei	SKM S1 S2 GBS8	Medium-grained granite	Weathering profile highly variable: slightly−moderately decomposed granite coreslabs within completely decomposed granite; coreslabs often bound by discontinuities steeply dipping into slope; exfoliation zones (5−15 mm) adjacent to joint sets often filled with kaolin and manganese oxide, pinkish white **silty clay** (SKM S1), light gray soft **clay** (SKM S2) or very soft, very dark grayish brown **sandy silty clay** and very soft, pale yellow **sandy silty clay** (SKM GBS8).
Sai Sha Road	SSR 1 5 7 9 DS1	Coarse ash crystal tuff	Partings occupied by somewhat poorly defined and discontinuous clay veins: not obviously original primary joints of shears, consistent with inherent heterogeneous nature of tuff; openings may have developed during weathering process; often irregular to diffuse contact with host rocks, black veins and lenses throughout, except SSR 7, cream/white **clay**
Fei Ngo Shan	FNS N (North) S (South)	Fine to coarse ash crystal tuff	Thin (~0.5-2 mm) veins within very thick (up to 35 m) saprolite, which they criss-cross in a 'box-work' structure, **texture not determined** (too thin).
Shum Wan Road	SWR S12N (North) S12W (West)	Eutaxic fine ash vitric tuff	Kaolin commonly accumulated after minor movements, hence shearing across discontinuities sub-parallel to slope; infilled kaolin acted as aquiclude, hence more kaolin infilling, soft reddish-yellow, also pink, **clay**.

* from S. Parry (pers. comm.), with some textural observations in extracted samples

quantitatively (Churchman *et al.*, 1984). Finer (1−2, 0.2−1, and <0.2 μm) fractions were also obtained from several samples. As a supplement to the XRD analyses, the cation exchange capacities (CECs) were determined for the clay and finer fractions of some samples. For this purpose, 80 mg of air-dried material was dispersed in deionized water and then deposited on a cellulose acetate filter with 0.2 μm pores. After saturation with a 1 M $BaCl_2$ solution, and washing free of salt and being oven dried, it was analyzed for all major elements, including barium, by X-ray fluorescence (XRF) spectroscopy. Barium is assumed to be absent from the untreated material but to have saturated exchange sites; its content therefore gives the CEC.

The DTA and TGA analyses were carried out together using a Rigaku TG-DTA apparatus equipped with infrared heating and also water-cooling (Thermflex 8100 series). Weighed whole sub-samples of ~20 mg were heated in platinum crucibles at a rate of 10ºC/min from ambient temperatures to 1050ºC. A quantitative analysis of kaolin mineral (kaolinite + halloysite) was made by measuring the sizes of the inflections in TGA at 520−560ºC in comparison with those for a pure kaolinite (Georgia kaolinite), following correction for the relative weights of the sample and standard samples.

In order that thin sections could be obtained of the samples for optical microscopy, the largely intact block of each of the samples that had been extracted from the field was first prepared following Salins and Ringroase-Vose (1994). The block sample was air-dried initially, dried in an oven at 40ºC, and impregnated with a CR64 clear, polyester embedding resin (Daystar Pty Ltd) (diluted with methyl methacrylate monomer in a resin: monomer ratio of 0.5, with a small quantity of cumene

hyperoxide catalyst added to keep the mixture liquid long enough for sample penetration and with the further addition of Uvtex OB fluorescent dye (Ciba-Geigy Pty Ltd) to aid identification under UV light). Following completion of polymerization, thin sections 70 mm × 50 mm in size were cut parallel in order to ensure representation of vein infill material and its immediate surroundings. These were photographed and their petrography described.

RESULTS

Microscopic descriptions of the host rocks

Examples of the altered host rocks are shown in Figure 1. Kaolinization occurs more readily from some parent minerals than from others. Feldspars in a sample from Tiu Keng Leng (TKL SP2E) (Figure 1a) showed alteration to kaolin whereas primary muscovite and quartz largely retain their original forms. A similar effect in the bulk rock at Sha Tin College (sample STC S1OppC) was noted (Figure 1b), where a large plagioclase crystal occupying most of the image is invaded by an early micro-network of the primary greisen alteration minerals sericite and quartz. The relict cores of plagioclase incorporated within this network are densely clouded by pervasive near-isotropic kaolin, interpreted to be later, supergene alteration. Kaolin is more distinctly coarse decussate/vermiform in part of the host rock sample TKL 3 (Figure 1c), where it is likely to have formed from muscovite in the original greisenized granite. Fe-stained kaolin formed from biotite occurs prominently alongside other altered fragments (Figure 1d) and also some quartz crystals within a network of clay particles from Sai Sha Road (sample SSR 1).

Early, primary greisen-related alteration generally occurred in the host rocks of TKL and STC granites, manifest as patchy micro-mosaics and stringers of sericite intergrown with very fine micro-prismatic quartz, commonly replacing original feldspar and muscovite crystals. This greisen alteration has been largely camouflaged by an overprint of later pervasive supergene/weathering alteration, which forms the saprolite. In the granite samples from Shek Kip Mei (not shown), and in the tuffs from Sai Sha Road and Fei Ngo Shan (not shown), no clear evidence emerges of primary alteration in bulk host rock prior to the current saprolite development.

Overall, kaolin alteration is ubiquitous and extensive throughout the host rocks studied. The result is a weakening of the rock fabric and an increase in its water-holding capacity. During weathering, additional

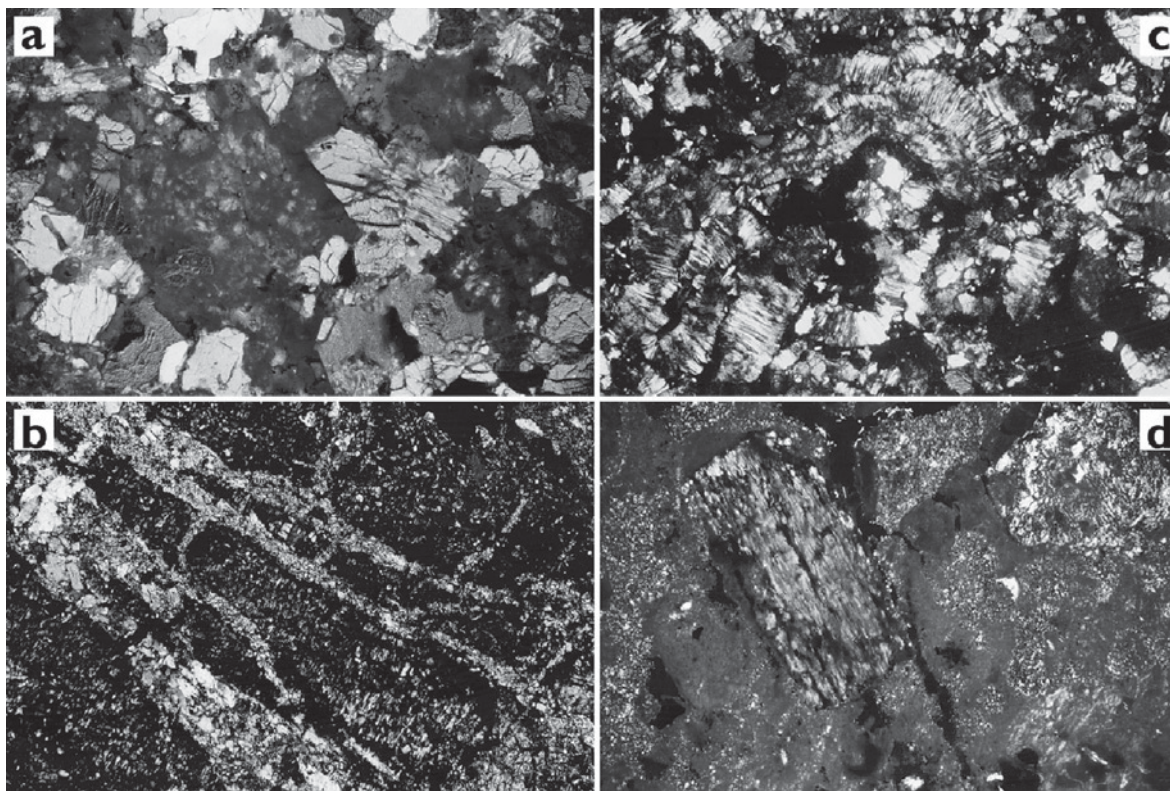

Figure 1. Photomicrograph examples of alteration within the matrix of host rocks: (a) granite, sample TKL SP2E, (b) granite, sample STC S1OppC, (c) granite, sample TKL 3, (d) tuff, sample SSR 1. The width of each photograph represents 6.75 mm.

discontinuities formed in the rock mass and these, together with the primary discontinuities, provided the host zones for the formation of kaolin-rich infill.

Macro-characteristics of the saprolites: host rocks including infill

Photographs of thin sections which show examples of host rock containing infill in various saprolites (Figure 2) and of block samples with similar examples (Figure 3) are shown. All infills could be characterized as either light or dark colored. As characterized in the field by S. Parry (pers. comm.), light colored infills were sometimes white (Munsell color of 10YR8/1, *e.g.* in SKM S1 and S2, Figure 2b:), but they could also show pink (7.5YR7/3, *e.g.* in TKL 2, TKL 2SP2E, Figure 2a, SWR S12N, Figure 2c, and SWR S12W), dappled

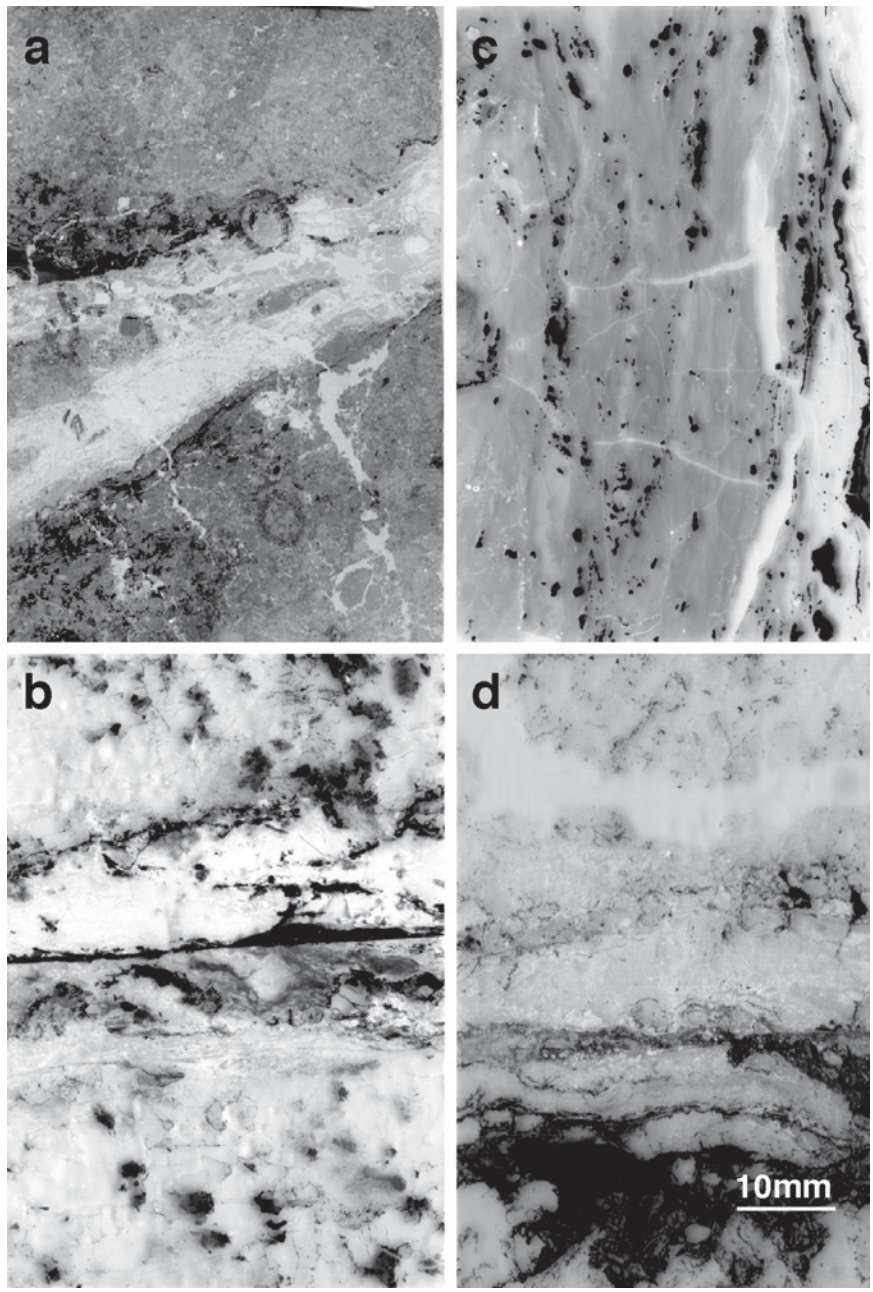

Figure 2. Photographs of thin sections of host rocks including infills: (a) sample TKL SP2E in granite, (b) sample SKM S2 in granite, (c) thin section of sample SWR S12N in tuff, (d) thin section of sample STC S1A in granite. The width of each photograph represents 46.5 mm.

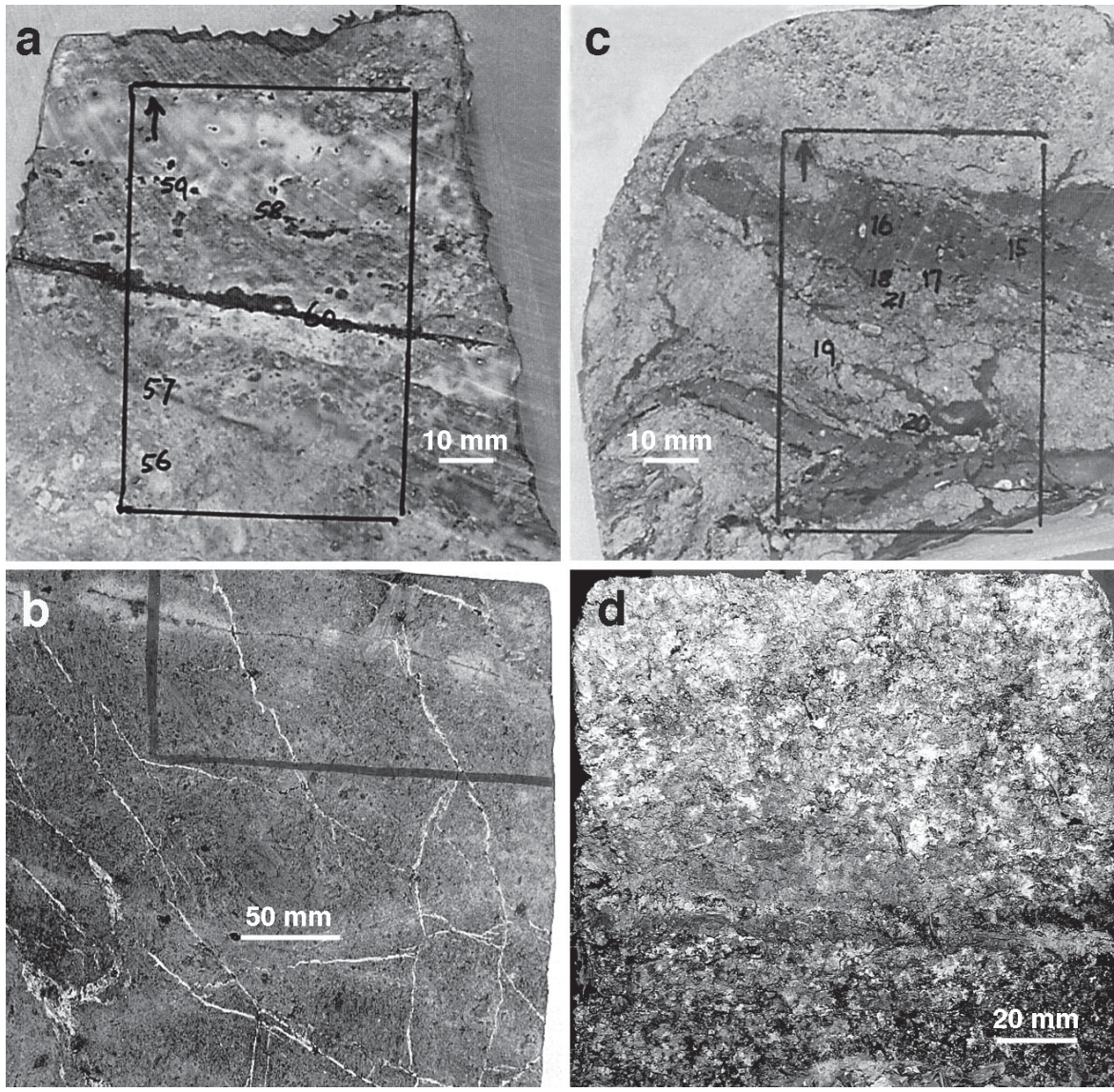

Figure 3. Photographs of block-sample host rocks including infills: (a) sample SSR DS1 in tuff, (b) sample FNS S in tuff; (c) sample TKL 3 in granite, (d) sample SKM GBS8 in granite.

yellow (10YR8/6, *e.g.* in all SSR samples, including SSR DS1, Figure 3a), or very pale brown (10YR7/3, *e.g.* in TKL2, SKM S1, and S2, Figure 2b) and similar colors, sometimes in different patches within the same infill. Field characterization (S. Parry, pers. comm.) also showed that dark-colored infills ranged from reddish-yellow (5YR6/8, *e.g.* in TKL 1 and 3, Figure 3c) through buff (7.5YR7/6, *e.g.* in SWR S12W), brown (7.5YR5/6, *e.g.* in FNS N), very dark grayish-brown (2.5YR3/2, *e.g.* in SKM GBS8, Figure 3d) to black (5Y2.5/1, *e.g.* in STC S1OppC and S1A, Figure 2d) and similar colors, also sometimes in different patches in the same infill.

Textures of infills (Table 1) were determined to be either clay (TKL 2 and SP2E and W, SKM S2, all SSR and SWR S12N and W) or silty clay (SKM S1) in the case of light-colored infills. Dark-colored infills ranged in terms of their textures from clay (SWR S12N and W), through silty clay (TKL 1 and 3) to the coarser grades of sandy, silty clay (SKM GBS8), and sandy silt (both STC).

Infills also varied in terms of their shapes and geometric relations to one another. Most were parallel or sub parallel within the same sample. The major exceptions were the two samples from Fei Ngo Shan, FNS N and S, where (light-colored) infills occurred as broad networks of intersecting veinlets, giving a 'box-work' effect (*e.g.* in FNS S, Figure 3b).

Infills also showed variations in thickness or width, mainly between samples, but sometimes also within

samples. Their widths varied from no more than 5 mm in the two FNS samples, to 40−55 mm, albeit sometimes as bifurcated veins, in the two STC samples. In some cases, infills appeared as adjacent parallel veins with contrasting colors. Hence the more common thicker, dark (buff)-colored vein was sometimes joined by a parallel, thinner, white-colored vein in samples SWR S12W, while the dominant thicker, dark (very dark grayish brown)-colored vein in SKM GBS8 was accompanied by a thinner, light (pale yellow)-colored vein (Figure 3d).

The nature of the contact between the infill and its surrounding host rock also varied, from quite sharp, *e.g.* in light-colored infills in TKL SP2E (Figure 2a), SKM S2 (Figure 2b), and FNS S (Figure 3b), to very diffuse, *e.g.* in dark-colored infill in STC S1A (Figure 2d).

Microtextures of infills

Examples of the internal fabric of infills are shown in Figure 4. The example of a light-colored infill from Tiu Keng Leng, sample TKL 2, shows infill only (Figure 4a). Many infills show a weak foliation probably associated with shear and deformation and this feature is shown in the core of the infill in Figure 4a. The example from Sai Sha Road, sample SSR DS1 (Figure 4b), shows the boundary between host rock and infill. Dark features that include Mn oxides occur throughout the infill in many of the samples, and are particularly prominent as continuous staining along one border of its host rock in the image shown in Figure 4b. Other infills from Sai Sha Road samples, not shown here, revealed indications of shearing.

Figure 4c,d, from Fei Ngo Shan, came from sample FNS N. The micro-fabric within the kaolin veins in the saprolite at this site ranges from massive cryptocrystalline, comprising very fine crystals (Figure 4c), to randomly disposed micro-vermiform (Figure 4d); both forms often occur as intimate mixtures within the same sample (FNS N, in this case). These kaolin infills generally show a random unstressed fabric with no clear evidence of shear or brecciation.

The example of a dark-colored infill from Tiu Keng Leng, sample TKL 1 (Figure 4e), displays a dominantly streaky-foliated fabric, which proved to be a common feature of reddish yellow infills from TKL 1 and 3 and also buff colored infills from SWR S12N and S12W. In the case of the two TKL samples with dark-colored infills, it was apparent that the weakly foliated infill often enclosed fine granular quartz, probably residuals from sheared and comminuted granitic host rock. The foliations are commonly disrupted, being cross-cut by what appear to be later, finer, and more random kaolin. These observations suggest shear structures filled by early kaolin, which have been subsequently dislocated and cemented by later generations of kaolin. Foliations which have also been disrupted may incorporate comminuted quartz and other primary minerals as breccia.

Typical features of the dark (black)-colored infill from the two sites at Sha Tin College are shown in Figure 4f. Apart from their color (black) and coarse textures (sandy silt), these samples are characterized by their bifurcating shape. They are sometimes foliated, as in the example (Figure 4f). Commonly, the black (manganiferous) infill is seen to permeate poorly defined bands of extensive fine host-rock breccia including finely comminuted quartz and other primary minerals, as illustrated (Figure 4f). Also in these zones, thin laminations of apparently early and relatively clear (white) cryptocrystalline clay have been dislocated, then filled between, and cemented by, later black Mn oxide.

Overall, most kaolin infill fabrics in the various samples are microscopically heterogeneous, with textural relations indicating generally more than one, and probably contiguous, generations of kaolin formation. Textures also suggest that shearing and deformation have occurred within the infill during the deposition of the clay, with these events likely to have initiated the onset of new stages of kaolin formation by precipitation from solution. In samples SKM GBS8 (Figure 3d) and also SWR S12W, infill heterogeneity is apparent at the macroscopic level, with lighter-colored infill occurring alongside and in parallel with dark infill. The Mn and/or Fe oxides appear here to have been oxidized in the course of forming the darker infills whereas the lighter infills formed subsequently from solutions containing little or no Mn or Fe.

The kaolin ± Mn oxide infill has formed primarily within discontinuities in the host rocks, some of which may be early shears either being primary, *i.e.* prior to weathering, or have resulted from shearing along discontinuities which may have already contained kaolin infill, as indicated by incorporated fine brecciated and comminuted host rock (or earlier kaolin) residuals.

Contents of kaolin minerals and quartz in infill

The amounts of quartz (from XRD of powdered samples), total kaolin (from TGA), and halloysite content as a percentage of total kaolin in the <2 μm fractions (from XRD of formamide-treated <2 μm fractions) of the various infills are listed in Table 2, classified by infill type. Within each category of infill, results for individual infills are arranged in descending order of their halloysite contents.

Infills, as analyzed, were mostly rich in kaolin minerals and contained little quartz, except for the irregular types of infills, *i.e.* the light-colored infills from Fei Ngo Shan and their dark counterparts from Sha Tin College, as well as the dark-colored infill in the SKM GBS8 sample from Shek Kip Mei (Table 2). Analyses of those from Fei Ngo Shan may be less reliable since the infills were extremely narrow (no more than 5 mm wide) (*e.g.* Figure 3b) and so were difficult to sample without contamination from surrounding rock. Infills from all sites other than those at Fei Ngo Shan

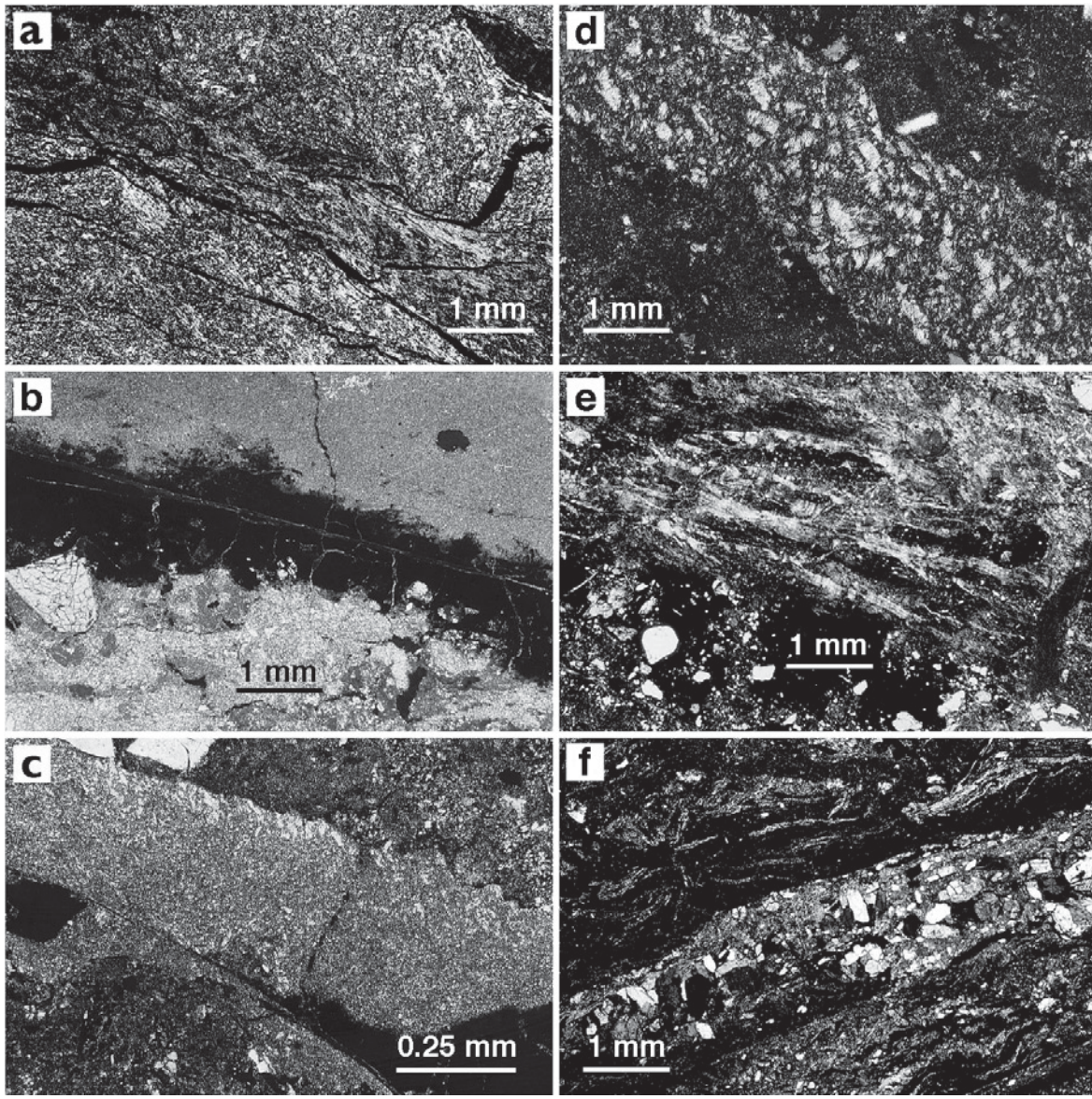

Figure 4. Photomicrographs illustrating typical micro fabrics of infills in samples: (a) TKL 2 in granite, (b) SSR DS1 in tuff, (c) FNS N in tuff, (d) FNS N in tuff, (e) TKL 1 in granite, (f) STC S1A in granite.

were at least 10 mm wide and more often $\geqslant$20 mm at their widest points and therefore their large quartz contents indicate the natural incorporation of this primary mineral in the infill.

Examples of the XRD analyses for the composition of the individual kaolin minerals, halloysite and kaolinite, and of other clay-sized minerals are shown in Figure 5. The kaolin contents of many of the light-colored infills were strongly halloysitic (*e.g.* TKL 2 from granite, Figure 5a), regardless of parent rock type (*e.g.* SWR S12W and S12N, from tuff – XRD patterns not shown), while others were strongly or mostly kaolinitic, which was the case for all samples from Sai Sha Road (*e.g.* SSR 5, Figure 5b), except for SSR 7, which comprised similar quantities of each of halloysite and kaolinite. Occasional occurrences of a micaceous phase were observed, most clearly evidenced by a peak near 10 Å in the (1) air-dried, (2) formamide-treated, and also, diagnostically, (3) oven-dried and glycerol-treated preparations of SSR 5 in Figure 5b. This phase was probably clay-size primary mica, present in a minor amount.

Dark-colored infills either contained mixed halloysite and kaolinite in roughly similar proportions or were highly kaolinitic. In the case of sample STC S1OppC (Figure 5c), a strong 9.5 Å peak also showed a substantial proportion of the Mn dioxide mineral,

Table 2. Contents of kaolin minerals and quartz in infill samples ordered in descending proportions of halloysite in their clay-size kaolin.

Sample	Rock type	Color of infill	Quartz (—— % of whole sample ——)	Kaolin	Halloysite (% of <2 μm kaolin)
TKL 2	Granite	Light	5, 20§	80, 90§	100
TKL SP2W	"	"	5, 20§	75	91, 97§
TKL SP2E	"	"	n.d.	75	81
SWR S12W*	Tuff	"	0	85	78
SWR S12N*	"	"	<1	90	78
SKM S1/2	Granite	"	10	65	71
FNS N	Tuff	"	25	65	65
FNS S	"	"	35	40	55
STC S1OppC	Granite	Dark	20	30	55
TKL 3**	"	"	20	n.d.	51
SSR 7	Tuff	Light	10	90	51
SKM GBS8	Granite	Dark	25	25, 30§	36, 38§
SSR 9	"	Light	<5	85	31, 35§
SSR 1	"	"	0, <1§	95	21, 27§
SSR DS1	"	"	5	80	21
SSR 5	"	"	5	90	13, 26§
STC S1A	"	Dark	15	25	21
SWR S12W†	Tuff	"	<1	80	17
SWR S12N†	"	"	<5	85	13

n.d.: not determined
*: white infill
**: no determinations for TKL1
†: 'buff' infill
§: duplicate sub-samples

todorokite. They may also have contained some comminuted primary minerals, as indicated by a shoulder on the low-angle side of the peak for todorokite in Figure 5c.

Morphology and size of particles of kaolin and other minerals in infill

Scanning electron micrographs (Figure 6) show examples of light-colored infills. Extremely long (>40 μm) fibers, identified under greater magnification as tubular, appear in the infill from some of the samples from Tiu Keng Leng (Figure 6a). The particle shapes are consistent with the occurrence of a particularly pure form of halloysite that was termed 'Patch clay' by Norrish (1995). The SEM images of light-colored infills in samples from Shek Kip Mei (Figure 6b) and Shum Wan Road (Figure 6c) show that they are dominated by long tubes (mostly ~2–4 μm long). The particular infill shown in Figure 6c derives from light-colored (white) infill in a sample (SKM S12N) in which the predominant infill, which adjoins the white infill, is dark colored (Figure 2c).

The SEM images of light-colored infills from Sai Sha Road (Figure 6d,e) generally show a dominance of platy particles within vermiform packets, consistent with their very kaolinitic compositions. The arrangement of particles in Figure 6d appears to resemble rosettes. Component platy particles in these arrangements are thin and show some curling so that particles are not strictly parallel with one another. Similarly randomly stacked, thin, curled, platy particles appear in other infills in samples from this location (*e.g.* Figure 6e, from sample SSR DS1), although they are not clearly rosette-like as in Figure 6d. A multiplicity of peaks in XRD traces of randomly oriented powdered samples from SSR infills (not shown) indicated that their component kaolinite was quite crystalline. The randomly stacked but very crystalline particles of kaolinite in the infills are consistent with formation by neogenesis from solution, as discussed below.

The infills in samples from Fei Ngo Shan (*e.g.* Figure 6f) showed mainly thin, curled, platy particles, ~1–2 μm in extent, in SEM. Often these were packed quite closely together. A highly magnified view (Figure 6f) of typical examples of these particles (from sample FNS S) revealed that some, at least, of these micrometer-sized particles are themselves composed of extremely small (<0.2 μm long) platy or fibrous particles joined together at their edges. Also noteworthy is that XRD peaks for kaolin minerals in FNS infills (not shown) are very broad. The small particle size is the likely cause of peak broadening, consistent with the observation in SEM (Figure 6f) of small particles forming into larger composites.

Scanning electron microscopy images (Figure 7) of dark-colored infills show, within the infill from a single

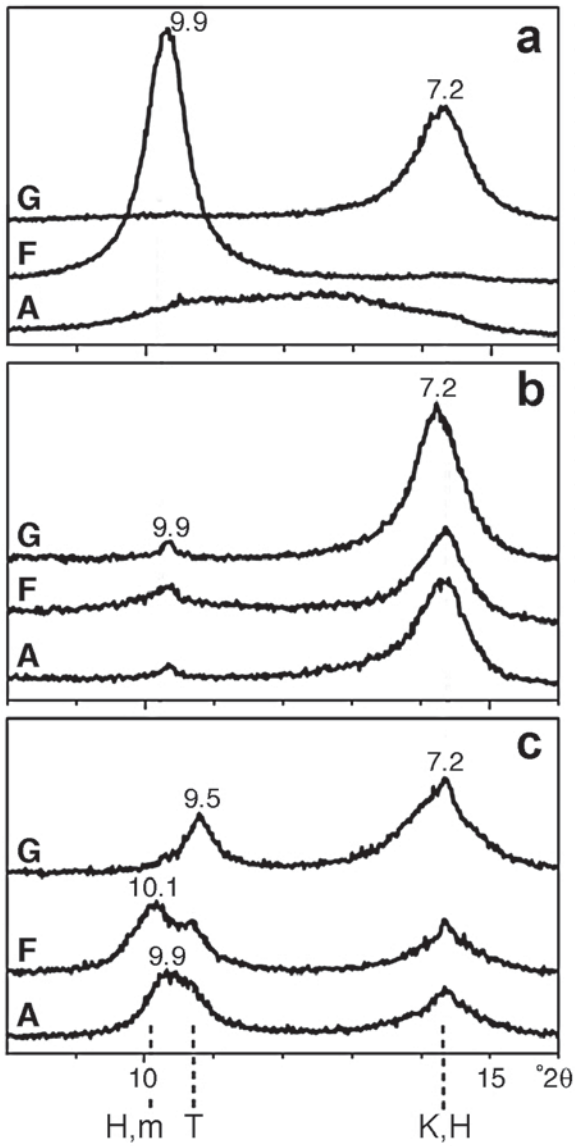

Figure 5. Basal spacing peaks in XRD patterns for sedimented infill of the <2 μm fraction sub-samples from (a) TKL 2, (b) SSR 5, and (c) STC S1OppC. Before XRD analysis, each sub-sample had been: A, air-dried; F, treated with formamide; or G, formamide-treated, heated at 105ºC, and then treated with glycerol (respective patterns from bottom to top in each set of three patterns). The vertical lines indicate diagnostic peak positions for: halloysite (H) and a micaceous mineral (m), after formamide treatment, both near 10 Å; kaolinite (K) after all treatments, together with H after oven-drying and glycerol treatment, both near 7 Å; and todorokite (T), after all treatments, at ~9.5 Å. Peak spacings are in Angstroms.

sample (TKL 3) (Figure 7a), a mixture of short (~0.5−1 μm long) fibrous particles with platy particles which are often ~1 μm long. Images also indicated that fibrous particles from other parts of this infill (not shown) are also generally longer (~2−4 μm long) and somewhat similar to those in white infill in other samples (*e.g.* Figure 6b). This is also true for isolated spots which have long fibrous particles of the 'Patch clay' type, similar to those shown for white infill from sample TKL 2 (Figure 6a). The infill in sample TKL 3 was especially heterogeneous. The dark (buff) infill from the SWR S12N sample, which also contains some white infill (Figures 2c, 6c), shows mainly small (generally 0.2−0.3 μm long) platy particles (Figure 7b) which are often hexagonal or pseudo-hexagonal in shape but do not occur in vermiform books. Some fibrous particles that are generally 0.5−1 μm long also occur.

The black infill in samples from Sha Tin College comprised a mixture of medium-length (~1−2 μm long) fibrous particles, together with platy particles which are of various sizes, including some that are <1 μm long and others that are ⩾2 μm long (*e.g.* Figure 7c). The infill in STC samples also contains a large amount of Mn oxide, however, which was shown by XRD to occur as todorokite. An area of accumulation of irregularly shaped, relatively large (generally >4 μm long) platy particles that were analyzed as virtually pure Mn, among cations, by EDX is shown in Figure 7d.

Occurrence of other minerals in infills

X-ray diffraction of powdered whole samples (not shown) showed that, apart from quartz (Table 2), few if any other primary rock minerals occurred in infill. Among other secondary minerals aside from kaolins, XRD of sedimented clay or finer fractions showed that, in addition to some mica (*e.g.* Figure 5b), a smectite phase occurred occasionally (in the infills from TKL 2 and SP2W, SSR 1 and 7, STC OppC, FNS S, and SWR S12W). However, the fine fractions in which these appeared all had small CEC values (<20, with most <10 $cmol_+kg^{-1}$) and comprised only very small proportions of the samples, such that smectite contents were all <~1% of whole infill. Gibbsite was also found as a minor component in the infill in one sample (TKL 3), and could also have been present in the related sample TKL 1, which was not analyzed by XRD.

As well as the clear XRD (Figure 5c) and SEM (Figure 7d) evidence for the Mn oxide todorokite in the STC samples, Mn was identified in significant amounts in two types of infill by EDX analyses carried out with SEM, *i.e.* (1) in black lenses alongside otherwise light-colored infills (*e.g.* Figure 2b, for SKM S2, Figures 3a, 4b, both for SSR DS1) and (2) in dark-colored infills. Black lenses were often discontinuous, however, *e.g.* in SKM S2, which also had veins that contained no such lenses, and not all dark-colored infills showed high concentrations of Mn. In particular, Mn occurred in high concentrations throughout the black infill in STC S1A (Figures 2d, 4f) and S1OppC, occasionally in the dark infill in SKM GBS8 (Figure 3d), and in the buff infill in SWR S12W (buff infill in SWR S12N was not analyzed). On the other hand, it was hardly detected in the 23 spots in dark-colored infill that were examined from TKL 3. Among other TKL samples, no Mn was found in 11 spots analyzed from

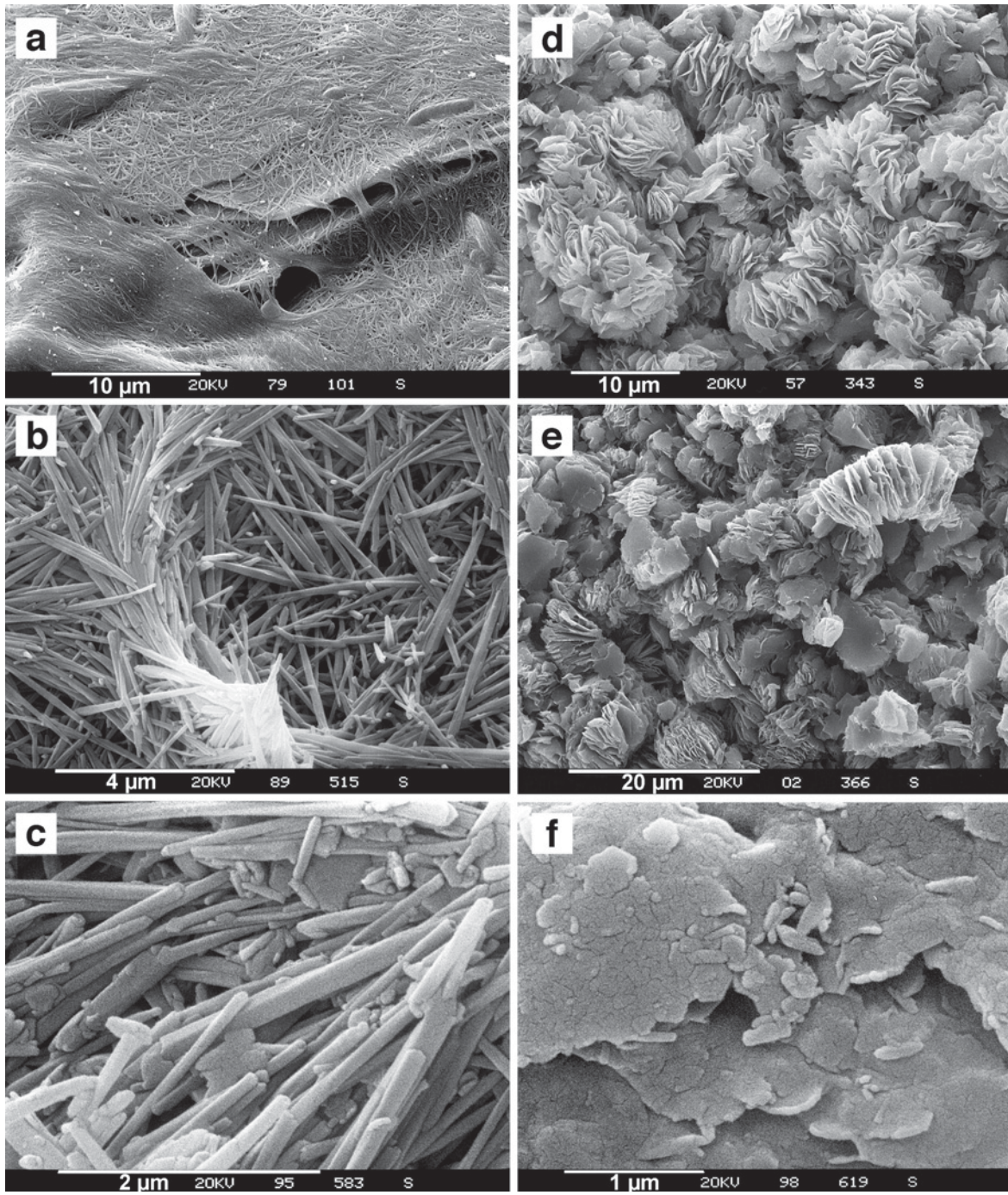

Figure 6. SEM images of examples of light-colored infills in samples: (a) TKL 2, at low magnification; (b) SKM S1, at high magnification, (c) SWR S12N, at very high magnification, (d) SSR DS1, at low magnification, (e) SSR 5, at low magnification, (f) FNS N, at very high magnification.

light-colored infill in TKL 2, but it occurred in just two of 17 spots in light-colored infill in TKL SP2E and in two of 15 spots in such infill in TKL SP2W. Manganese was not detected in light-colored infill in FNS S (ten spots analyzed) and N (seven spots analyzed). While it was present in black veins alongside light-colored infill in SSR 1, 5, and DS1, it was only occasionally detected in light-colored infill in SSR 7 and 9.

The XRD patterns of powdered whole samples revealed goethite in dark-colored infill in TKL 3. XRD

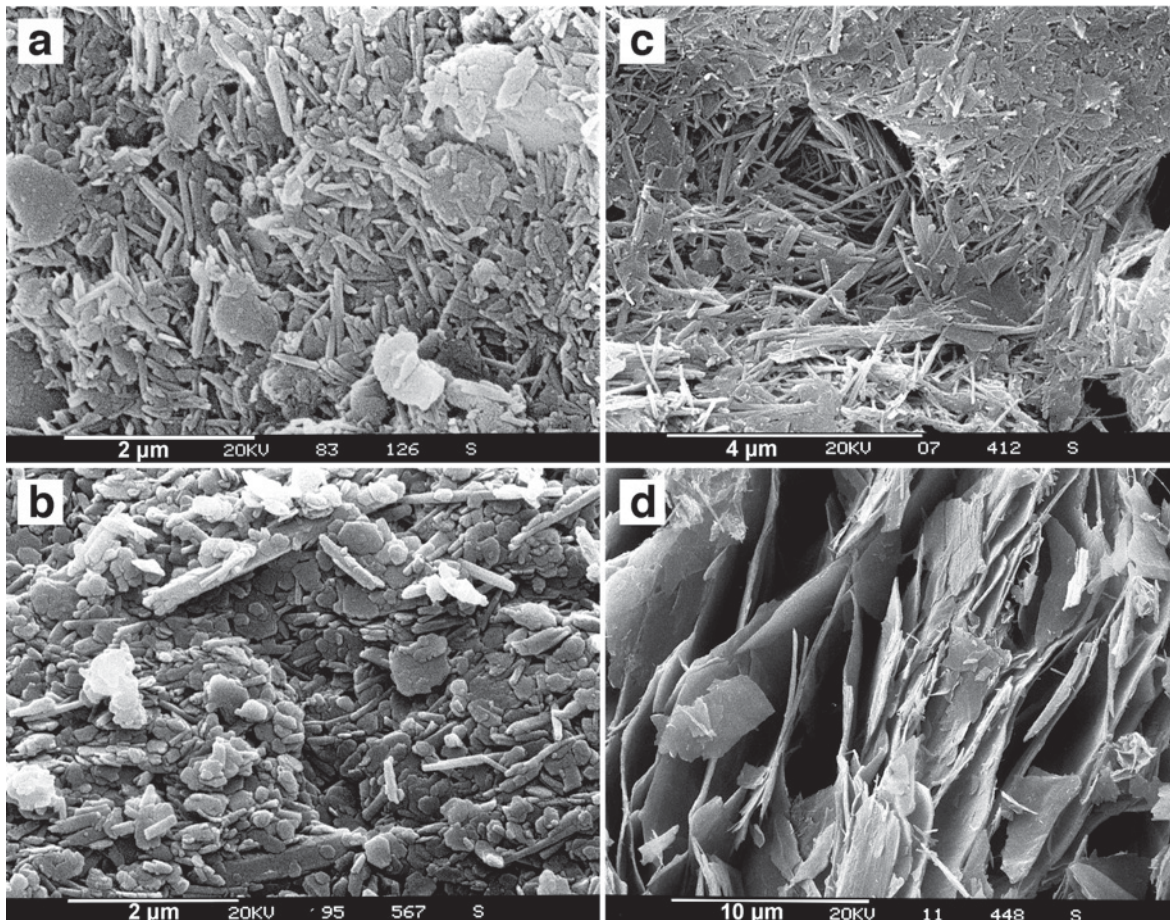

Figure 7. SEM images of examples of dark-colored infills in: (a) TKL 3, at very high magnification, (b) SWR S12N, at very high magnification, (c) STC S1A, at high magnification, (d) STC S1OppC, at low magnification.

peaks for Fe oxides were not obvious in other samples but EDX, while confirming that the Fe content was high in dark infills in TKL 3 (and also TKL 1), showed that it was not particularly high in any other infills except for the buff infill in SWR S12W (buff infill in SWRS12N was not analyzed) and the dark infill in SKM GBS8. Significant occurrences of Fe were also detected in some parts of white infill in TKL SPSE (five of 17 spots) and in TKL SP2W (eight of 15 spots).

DISCUSSION

The mineralogical and morphological properties of the kaolin minerals in relation to the characteristics of the infills in which they occur are summarized here (Table 3). In the context of the aims of this work, to discover the important factors governing the formation of either halloysite or kaolinite, the kaolin-rich infills at the various sites varied above all in: (1) their color and texture, (2) the sizes and shapes of their particles, and (3) their halloysite and kaolinite contents and the occurrence of other minerals.

Explanations of each of the three diagnostic features of infills follow, referring to Table 3 unless otherwise noted.

Origin of the colors and textures of the different infills

Manganese occurred in high concentrations in all samples of dark-colored infill that were analyzed except for TKL 3. Undoubtedly, the Mn contributes to their dark color, most notably to the black infills of the STC samples. While little or no Mn was detected in TKL samples and it was detected only occasionally in the buff-colored SWR infill, in the very dark grayish brown infill in SKM GBS8, and in the infill in TKL 3, which was reddish-yellow in color. All of these, however, showed large concentrations of Fe throughout their infills and its presence probably causes or certainly contributes to the dark color in these cases.

With the exception of FNS infills, which were exceptional because of their non-parallel shape, suggesting, along with other observations, a non-weathering origin (see next sub-section), all light-colored infills had fine (clay or silty clay) textures (Table 1). Generally,

Table 3. Characteristics of the infills and their kaolin minerals, leading to grouping of infills by kaolin mineralogy and morphology.

Sample	Color (L = light, D = dark)	Mn (high concentrations in EDX analyses)	Fe (high concentrations in EDX analyses)	Kaolin (% of whole sample)	Halloysite (% of total kaolin minerals)	Length of dominant particles (μm)	Dominant particle shapes	Group
TKL2	L	–	–	85*	100	>40	Long, fibrous bunches	Halloysite large crystals
TKLSP2E	L	o	o	75	81	3–4, 10–20	Long tubes; long fibrous bunches	
TKLSP2W	L	o	o	75	94*	3–4	Long tubes	
SKM S1/S2	L	o	–	65	71	2.5–3.5	Medium-length tubes	
SWR S12N white	L	–	–	90	78	1.5–6.5	Medium–long tubes	
SWR S12W white	L	–	–	85	78	0.7–3.5	Small–medium tubes	
SSR 1	L	V	–	95	24*	1.5–6.5	Vermiform plates	Kaolinite large crystals
SSR 5	L	V	–	90	20*	0.5–5	Vermiform plates	
SSR 7	L	o	–	90	51	1.5–3	Vermiform plates	
SSR 9	L	o	–	85	33*	1–6	Vermiform plates	
SSR DS1	L	V	–	80	21	3–10	Vermiform plates, often in rosettes	
FNS N	L	–	–	65	65	0.5	Composites of very short fibers and plates	Mixed very small crystals
FNS S	L	–	–	40	55	0.4–0.6	Composites of very short fibers and plates	
TKL3	D	–	T	?	51	0.3–1.5	Short-medium tubes and plates	Mixed small crystals
STC S1A	D	T	–	25	21	0.7–1.1	Plates and (thick) tubes	
STC S1OppC	D	T	–	30	55	0.5–3	Plates and (thick) tubes	
SKM GBS8	D	o	T	30*	37*	0.3–1.3	Short flat fibers and small plates	
SWR S12N buff	D	?	?	85	13	0.2–0.3	Small hexagonal plates	Kaolinite small crystals
SWR S12W buff	D	o	T	80	17	0.2–0.3	Small hexagonal plates	

– not, or hardly, detected; o – occasional; V – in separate black veins or lenses; T – throughout main infill; ? – not analyzed; * – means of duplicates

they also had small quartz contents (Table 2). Dark-colored infills, on the other hand, had either fine textures (TKL 1 & 3, and SWR samples) or else coarse textures (sandy silty clay for SKM GBS8 or sandy silt for STC samples). Generally, the latter had larger quartz contents than the former (although the differences were not always clear-cut) and also than the light-colored infills.

A schematic representation of the main processes which are likely to have occurred at the macroscopic level in the saprolites (Figure 8) helps explain the origin of the different color and texture of the various infills apart from those at Fei Ngo Shan (see next sub-section) and can also help to explain the different sizes and shapes of the kaolins formed (next sub-section). Fresh rock (1), containing discontinuities such as tectonic cooling or stress relief joints, has undergone alteration by weathering (and/or hydrothermal action) to give altered rock (2) in which the most easily altered primary minerals have been replaced by secondary minerals formed largely by neogenesis out of solution *in situ*. The rock became weakened through alteration, and deformation occurred, either through intergranular contacts (3a), or else by shearing (3b), although fracturing of unaltered rock could also have occurred (dashed lines). In the latter case, alteration would follow deformation. Secondary minerals, which are primarily kaolin minerals, have been formed by neogenesis from solution in the discontinuities. In case 3a, the disintegration of the rock at contacting edges of the discontinuity led to brecciation, producing a coarse-textured infill, and the breakdown of primary minerals in breccia within the discontinuity that is discolored mainly by Mn, but sometimes Fe, as an alternative or in addition to Mn (4a). Secondary minerals, including kaolins but sometimes also todorokite and also poorly ordered Mn oxides, formed by neogenesis within this chemically heterogeneous discontinuity. In case 3b, secondary minerals formed by neogenesis from solution within either a relatively chemically clean discontinuity, to give a light-colored and fine-textured infill, or, as in the case of the buff infills in SWR S12N and W, an infill that became discolored and chemically heterogeneous by dissolved impurities, especially compounds of Fe (4b).

Origins of the different sizes and shapes of kaolin particles

Common features of these properties have enabled the kaolin minerals in different infills to be sorted into five groups: halloysite large crystals; kaolinite large crystals; mixed very small crystals; mixed small crystals; and kaolinite small crystals; as shown in Table 3.

Halloysite large crystals group. The predominant halloysite in the light-colored infills from the samples at Tiu Keng Leng (from granite), apart from TKL 3, from Shek Kip Mei (also from granite), apart from SKM GBS8, and from Shum Wan Road (from tuff) generally appears as long tubular particles. In some cases these include very long, parallel, tubular particles within bunches that are similar to the 'Patch clay' of Norrish (1995), which is considered to be a very pure form of halloysite. 'Patch clay' in its type occurrence in Australia occurs as very pale white-blue translucent

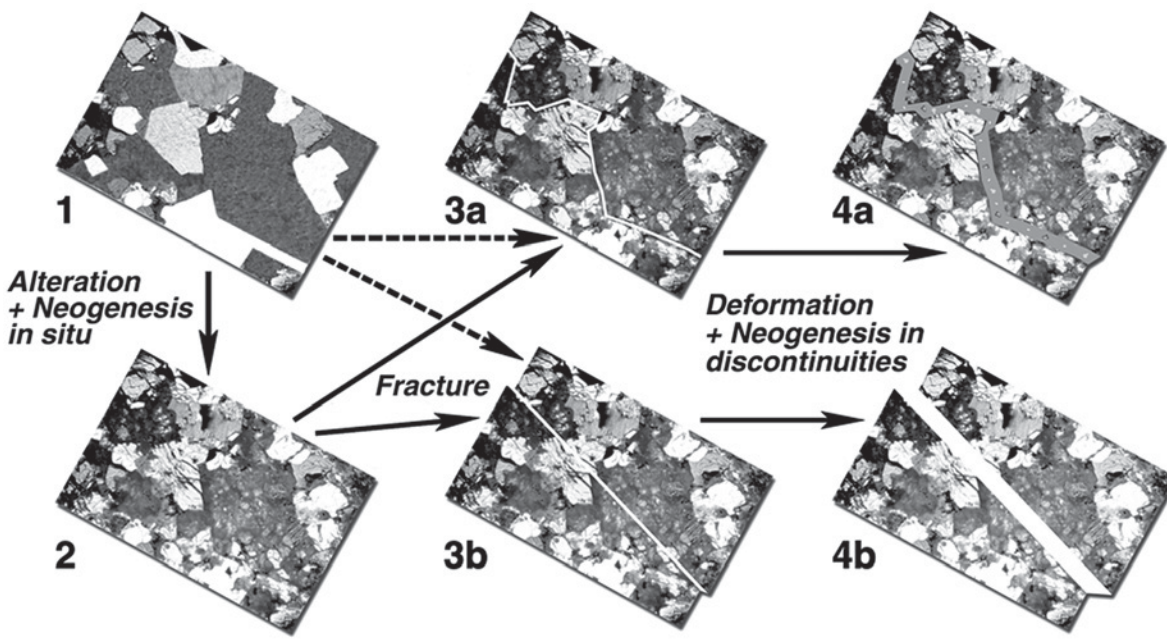

Figure 8. Schematic representation of the main processes likely to have occurred at the microscopic scale in the saprolites.

plastic clay within deeply weathered greenstones below a thick lateritic cap (Norrish, 1995) and apparently formed in an environment that was relatively unconstrained physically and was chemically quite free of impurity solutes (Norrish, 1995, and pers. comm.). The infill in TKL 2 (Figure 6a) and TKL SP2N and SP2W, and also part of TKL 3 infill (not shown) in which 'Patch clay'-like halloysite formed, appears to have provided a similarly unconstrained and pure environment for the synthesis of this type of crystal form of halloysite. Tubular particles contain less structural Fe than platy or pseudo-platy particles of halloysite and the lengths of tubular particles tend to decrease as Fe content in the structure increases (Churchman and Theng, 1984; Noro, 1986; Bailey, 1990). 'Patch clay' halloysite had almost no structural Fe (Norrish, 1995). Even the more conventionally long tubular forms of halloysite in the other light-colored infills at these two sites probably formed in a relatively pure environment, such as the type of discontinuity pictured as 4b in Figure 8, but which is uncontaminated by dissolved impurities.

Kaolinite large crystals group. The infill in samples from Sai Sha Road (from tuff) is generally highly kaolinitic. The kaolinite in this infill is largely composed of relatively large platy particles in vermiform packets.

Kaolinite in the form of vermiform books is extremely common in altered rocks (*e.g.* Sand, 1956; Moore, 1964; Jonas, 1964; Bates, 1971; Keller and Hanson, 1975; Keller, 1976, 1977; Senkayi *et al.*, 1984). Vermiform books of kaolinite do form directly from micas according to Jonas (1964) and Bates (1971); though the books are generally stacked in parallel, they have rough edges, the secondary kaolinite and primary mica are interleaved, and the kaolinite formed is of the *b* axis-disordered variety (Jonas, 1964). Vermiform books of kaolinite also form when alteration of feldspars occurs (Sand, 1956; Keller and Hanson, 1975; Keller, 1977).

The books that are neoformed in infills at Sai Sha Road are characterized by random stacking (Sand, 1956; Jonas, 1964; Bates, 1971; Keller, 1977), and their constituent kaolinite is generally very crystalline (Jonas, 1964; Senkayi *et al.*, 1984). Note that:

(1) the arrangement of 'books' in SEMs from the infills in the 'kaolinite large crystals' group was always random.

(2) EDX analyses of infills from all areas in the 'kaolinite large crystals' group contained essentially no K, indicating a lack of any mica in the vermiform stacks.

(3) XRD analyses show the kaolinite in these vermiform stacks to have high crystalline order.

Such evidence strongly suggests that kaolinite in the type of vermiform stacks seen in SSR infill samples formed out of solution, rather than by pseudomorphic replacement of mica in the solid state. The breakdown of feldspars is likely to have made an important contribution to the solutes from which vermiform kaolinite particles formed. By contrast, some kaolin formed within the host rock appears to be pseudomorphic after muscovite (Figure 1c).

Similar to the light-colored but strongly halloysitic infills at Tiu Keng Leng and Shum Wan Road, the infills at Sai Sha Road are suggested to have formed in relatively pure environments conducive to essentially unrestricted crystal growth. The infills probably originated in discontinuities such as that pictured as 4b in Figure 8, albeit uncontaminated by dissolved impurities.

Mixed very small crystals group. Particles, of both halloysite and kaolinite, in infills from the two samples from Fei Ngo Shan show unusual shapes in the form of thin, curled, platy entities that are probably composites of very small particles joined together. This infill material may have formed by a different process from that in other samples. A hydrothermal origin is possible in Hong Kong, especially in the vicinity of fault zones (Irfan, 1996) and in this sample the appearance of the kaolin minerals in some optical micrographs (*e.g.* Figure 4d) in randomly oriented (decussate) microvermiform configurations is consistent with a hydrothermal origin.

According to Keller (1976), a hydrothermal origin for clays is suggested by the occurrence of characteristic, high-temperature phases, especially alunite and cristobalite. Neither of these phases was identified in any of the samples in this study. Nonetheless, hydrothermal kaolins can be further characterized, according to Keller (1976), by a texture composed of relatively small flakes and/or elongates that are tightly packed and randomly interlocked. In the case of hydrothermal kaolinite, the plates occur as singles, sheaves, or thin packets, rather than the expansive books (Keller, 1976) which are characteristic of most of the kaolinite in samples in the present study. The products of alteration in the infill at Fei Ngo Shan (*e.g.* Figure 6f) commonly comprise thin sheets with close packing, and they are generally interlocked.

By contrast, weathering tends to give a loose arrangement of particles. The difference comes about because hydrothermal solutions alter the assemblages of primary minerals from the inside out as well as the outside in. Clays have a smaller bulk density than primary minerals so the volume of the solids increases upon alteration and hence a tightly packed mass is produced. However, weathering proceeds from the outside surfaces inward and the associated downward movement of solutions carries away dissolved products, leaving loose arrangements. The evidence discussed here suggests that the kaolin in infill at Fei Ngo Shan probably has a hydrothermal origin. With this possible exception, kaolin infills in the samples investigated probably formed by weathering.

Mixed and kaolinitic small crystals and very small crystals groups. Most of the infills with the shorter and

less well formed particles of kaolinite together with halloysite are dark-colored. A comparison of the kaolins in the two groups characterized by small crystals with those in the two groups characterized by large crystals suggests that the presence of brecciated rock and/or dissolved impurities such as Mn and Fe, led to a more complex and less clean chemical environment for crystal growth within infills in the former group than in the latter. Referring to Figure 8, small kaolin crystals have formed in either a type 4a discontinuity or a type 4b discontinuity which incorporated dissolved Fe and/or Mn at the time of their formation. A 'dirtier' environment has led to smaller crystals.

Furthermore, while the larger parts of the light-colored infills in TKL SP2E and SP2W and also SKM S2 showed large crystals, Mn, and sometimes also Fe, was found in parts of the infills in these samples. Scanning electron micrographs of the areas with enhanced Mn, in particular, revealed generally smaller and sparser tubular particles, but more platy particles, than appeared in the rest of the infill that was examined. Clearly the purity of the local infill environment in which kaolin minerals were formed dictated the resulting sizes, at least of the particles formed. Furthermore, the occurrence of bunches of long parallel fibrous particles in part of the infill in sample TKL 3 alongside both small platy particles and also medium-length fibrous particles in other parts of infill in this sample, confirmed the indications at the optical microscope scale (*e.g.* Figure 4a, for TKL 2) that multiple deformation events occurred. Each of these events led subsequently to new phases of generation of kaolin minerals, sometimes leading to heterogeneity in the products formed.

Origin of halloysite in comparison with kaolinite

When the characteristics of the infills that have resulted in pure or relatively pure halloysites through neogenesis, *i.e.* those in the 'halloysite large crystals' group in Table 3, are compared with the characteristics of those infills in which neogenesis has led to strongly kaolinitic products, *i.e.* the 'kaolinite large crystals' group, a major difference is that Mn is widespread throughout the strongly kaolinitic group but wholly or mostly absent from the strongly halloysitic group. Whereas Mn and/or Fe pervade the dark-colored infills belonging to the 'mixed small crystals' and 'kaolinite small crystals' groups (Table 3), white infills, such as those from Sai Sha Road, often include black spots, streaks, or veins which usually indicates Mn oxides. The occurrence of Mn – and sometimes also Fe – indicates that drying has occurred at some stage during the history of development of the infills containing these elements as oxides or oxyhydroxides. In contrast, the absence, or only occasional occurrence, of Mn and Fe from infills of the 'halloysite large crystals' group means that these have not dried to any extent or for any significant period of time during their development.

All the sample sites are very close together and can therefore be considered as having received similar amounts of precipitation during their weathering history. Infills, or parts of infills, have, however, dried to a greater extent in some samples than in others. The differences may reflect differences in the extent of drainage that has occurred in the different samples. Where Mn oxide occurs in veins along infill boundaries, as in many of the SSR samples, rapid drainage along the relict joints may have led to a dried and oxidized zone along the margin of the infill. Where Mn and/or Fe was detected in spots or streaks throughout infill, it may reflect enhanced drainage arising from the dislocation of earlier generations of kaolin within infill by later generations of the mineral type.

Dark infills containing larger particles of primary minerals from brecciation of the rock (*e.g.* Figure 4f) not surprisingly drain more rapidly than white infills comprising only secondary clay-size minerals (*e.g.* Figure 4a). This is consistent with dark infills having greater contents of kaolinite than of halloysite (Table 3). However, some white infills, and particularly those from the SSR site, also incorporate considerable Mn oxide in black bands or lenses (Table 3, also Figure 4b, for an example). The SSR samples have all derived from coarse ash tuff (Table 1). A coarse texture would allow fast drainage from the saprolite and from its boundary with newly formed infill. While the white infill in TKL samples have also formed from coarse-textured saprolite, which is granitic in this case (Table 1), coarse-textured tuff appears to be more easily drained than coarse-textured granite. The comparatively easy drainage of the coarse-textured tuff at the SSR site is consistent with the relatively larger amount of kaolinite compared with halloysite in infills formed in saprolite at this site.

Thermodynamic data suggest that kaolinite is more stable than halloysite. However, studies of weathering in relation to depth in profiles encompassing various degrees of altered rock and soils (Eswaran and Wong, 1978 – in Malaysia; Calvert *et al.*, 1980 – in North Carolina; Churchman and Gilkes, 1989 – in Western Australia; Churchman, 1990 – in New Zealand; Irfan, 1996 – in Hong Kong; Jeong, 2000 – in Korea) have shown that halloysite appears at an earlier stage of rock alteration than kaolinite. Studies of several Spanish soils by transmission electron microscopy (Romero *et al.*, 1992) indicated that kaolinite takes longer to develop than halloysite.

Kaolinite was found in higher, drier parts of weathering profiles in Western Australia (Churchman and Gilkes, 1989). The upper parts of these lateritic profiles are particularly dry. While this suggests that drier conditions favor kaolinite over halloysite, kaolinite is also favored over halloysite in the upper parts of weathering profiles studied in the tropical and subtropical environments of Malaysia (Eswaran and Wong, 1978) and Hong Kong (Irfan, 1996). Wet conditions

apparently are required for the formation of halloysite, due, probably, to its essential structural, *i.e.* interlayer, water (Churchman and Carr, 1975). Kaolinite may also be formed under wet conditions where strong alteration of primary minerals occurs. Nevertheless, where drying occurs, even if only seasonally, kaolinite is more likely to form than halloysite. Within the infills in Hong Kong saprolites, each of these minerals has formed under the most appropriate conditions for its neogenesis; no evidence was found for the transformation of one to the other.

Origin of smectite and gibbsite

Smectite occurred, in small amounts, in infills with the least efficient drainage, *i.e.* TKL 2 and SP2W, SWR S12W, and FNS S. Smectite often forms when drainage is retarded, allowing the build-up of Si and Mg, particularly, in solution (*e.g.* Churchman, 2000). It also occurred in SSR 7, and, most anomalously, in SSR 1, where Mn oxides were most evident, presumably because of good drainage. However, infills were not homogeneous and micro-sites within infills could have provided the appropriate conditions for its formation in these cases.

Gibbsite was identified in infills in sample TKL 3 only. Gibbsite formation is promoted by strong leaching and hence good drainage. The appearance of Fe oxides in infill in TKL 3 (Table 3) suggests that strong oxidation has occurred as a result of good drainage.

CONCLUSIONS

Saprolites on either granite or volcanic tuff that incorporated kaolin-rich infill veins were sampled from six separate hillside sites in Hong Kong. At one site only, hydrothermal alteration resulted in small, tightly packed particles of kaolin minerals within non-parallel infills. Otherwise, weathering led to concentrations of kaolin minerals in parallel or sub-parallel infills. On these sloping sites, this occurred by the following steps:

(1) The original rock was altered and clay minerals, mainly kaolin, were formed by neogenesis within the rock matrix;

(2) within the weathered rock, open cracks, *i.e.* discontinuities, appeared and/or shear zones developed;

(3) clay minerals, mainly kaolin, formed within discontinuities, leading to infills, resulting in

(4) dilation of the discontinuities; and

(5) further deformation, followed by further neogenesis within the expanded discontinuities.

Neogenesis of kaolins in open discontinuities led to light-colored infills. Shearing of the host rock led to the incorporation of primary minerals within dark infills. The occurrence of Mn and Fe oxides as break-down products of primary minerals in these infills and also in pure form in bands, spots, and lenses within white infills indicates that drying had occurred.

Large particles of either halloysite or kaolinite, with high degrees of crystalline order, formed in light-colored infills. They were largely monomineralic. Kaolin minerals that formed in dark infills, and in darker areas within otherwise white infills, tended to be smaller than those within the bulk of the white infills.

The formation of kaolinite rather than halloysite was favored where drying had occurred.

The overall conclusions are, therefore, that:

(1) the persistent presence of water is necessary for the formation of halloysites;

(2) under otherwise similar environmental and chemical conditions, kaolinites are formed rather than halloysites where drying occurs; and

(3) either halloysites or kaolinites form in larger particles when soluble impurities are absent in the solutions for their neogenesis.

ACKNOWLEDGMENTS

The authors thank the following former and current members of the staff of CSIRO Land and Water: Greg Rinder and Mary-Anne Fiebig, for skilful preparation of many of the figures; Jenny Anderson, Daniel Weissmann, and Adrian Beech (and his staff), for much of the laboratory work; Mark Raven for some of the photography; and Anthony Ringroase-Voase and Inars Salins for resin impregnation of the block samples. They are also grateful to Steve Parry, formerly of the Geotechnical Engineering Office of the Civil Engineering Department, Hong Kong, for samples and their field description and for his active interest in the work. Permission was granted by the Director of Civil Engineering and Development and the Head of the Geotechnical Engineering Office, Government of the Hong Kong Special Administrative Region, China, to enable the submission of this paper for publication.

REFERENCES

Bailey, S.W. (1990) Halloysite – a critical assessment. In: Proceedings of the 9th International Clay Conference, Strasbourg, Volume II (V.C. Farmer and Y. Tardy, editors). *Science Géologiques*, **86**, 89–98.

Bates, T.F. (1971) Kaolin minerals Pp. 109–157 in: *The Electron Optical Investigation of Clays* (J.A. Gard, editor). Monograph **3**, Mineralogical Society, London.

Bates, T.E., Hildebrand, F.A., and Swineford, A. (1950) Morphology and structure of endellite and halloysite. *American Mineralogist*, **6**, 237–248.

Bordallo, H.N., Aldridge, L.P., Churchman, G.J., Gates, W.P., Telling, M.T.F., Kiefer, K., Fouquet, P., Seydel, T., and Kimber, S.A.J. (2008) Quasi-elastic neutron scattering studies on clay interlayer-space highlighting the effect of the cation in confined water dynamics . *Journal of Physical Chemistry C*, **112**, 13982–13991.

Calvert, C.S., Buol, S.W., and Weed, S.B. (1980) Mineralogical transformations of a vertical rock-saprolite-soil sequence in the North Carolina Piedmont. *Soil Science Society of America Journal*, **44**, 1096–1112.

Campbell, S.D.G., Koor, N.P., Franks, C.A.M., and Shum, W.L. (1998) Geological assessment of slopes in areas close to major landslides on Hong Kong Island. Pp. 121–128 in: *Proceedings of the annual seminar on slope engineering in Hong Kong* (K.S. Li, J.N. Kay, and K.K.S. Ho, editors).

Balkema, Rotterdam.
Carter, J.R., Hatcher, M.T., and Di Carlo, L. (1987) Quantitative analysis of quartz and cristobalite in bentonite clay based products by X-ray diffraction. *Analytical Chemistry*, **59**, 513–519.
Churchman, G.J. (1990) Relevance of different intercalation tests for distinguishing halloysite from kaolinite in soils. *Clays and Clay Minerals*, **38**,5, 91–599
Churchman, G.J. (2000) The alteration and formation of soil minerals by weathering. Pp. F3–F76 in: *Handbook of Soil Science* (M.E. Sumner, editor). CRC Press, Boca Raton, Florida, USA.
Churchman, G.J. and Carr, R.M. (1975) The definition and nomenclature of halloysites. *Clays and Clay Minerals*, **23**, 382–388.
Churchman, G.J. and Gilkes, R.J. (1989) Recognition of intermediates in the possible transformation of halloysite to kaolinite. *Clay Minerals*, **24**, 579–590.
Churchman, G.J. and Theng, B.K.G. (1984) Interactions of halloysites with amides: Mineralogical factors affecting complex formation. *Clay Minerals*, **19**, 161–175.
Churchman, G.J., Whitton, J.S , Claridge, G.G.C., and Theng, B.K.G. (1984) Intercalation method using formamide for differentiating halloysite from kaolinite. *Clays and Clay Minerals*, **32**, 241–248.
Eswaran, H. and Wong Chaw Bin (1978) A study of a deep weathering profile on granite in Peninsular Malaysia. Parts I, II and III. *Soil Science Society of America Journal*, **42**, 144–158.
Irfan, T.Y. (1996) Mineralogy, fabric properties and classification of weathered granites in Hong Kong. *Quarterly Journal of Engineering Geology*, **29**, 5–35.
Irfan, T.Y. (1998) Structurally controlled landsides in saprolitic soils in Hong Kong. *Geotechnical and Geological Engineering*, **16**, 215–238.
Jackson, M.L. (1956) *Soil Chemical Analysis – Advanced Course.* Published by the author, Department of Soil Science, University of Wisconsin, Madison, WI, USA.
Jeong, G.Y. (2000) The dependence of localized crystallization of halloysite and kaolinite on primary minerals in the weathering profile of a granite. *Clays and Clay Minerals*, **48**, 196–203.
Jonas, E.C. (1964) Petrology of the Dry Branch, Georgia kaolin deposits. *Clays and Clay Minerals*, **12**, 199–205.
Joussein, E., Petit, S., Churchman, J., Theng, B., Righi, D., and Delvaux, B. (2005) Halloysite clay minerals – a review. *Clay Minerals*, **40**, 383–426.
Keller, W.D. (1976) Scan electron micrographs of kaolins collected from diverse environments of origin – 2. *Clays and Clay Minerals*, **24**, 201–204.
Keller, W.D. (1977) Scan electron micrographs of kaolins collected from diverse environments of origin – 4. *Clays and Clay Minerals*, **25**, 311–345.
Keller, W.D. and Hanson, R.F. (1975) Dissimilar fabrics by scan electron microscopy of sedimentary versus hydrothermal kaolins in Mexico. *Clays and Clay Minerals*, **23**, 201–204.
Kirk, P.A., Campbell, S.D.G., Fletcher, C.J.N., and Merriman, R.J. (1997) The significance of primary volcanic fabrics and clay distribution in landslides in Hong Kong. *Journal of the Geological Society, London*, **154**, 1009–1019.
Moore, L.R. (1964) The *in situ* formation and development of some kaolinite microcrystals. *Clay Minerals Bulletin* **5**, 338–352.
Newman, R.H., Childs, C.W., and Churchman, G.J. (1994) Aluminium coordination and structural disorder in halloysite and kaolinite by ^{27}Al NMR spectroscopy. *Clay Minerals*, **29**, 305–312.
Noro, H. (1986) Hexagonal platy halloysite in an altered tuff bed, Komaki City, Aichi prefecture, Central Japan. *Clay Minerals*, **21**, 401–415.
Norrish, K. (1995) An unusual fibrous halloysite. Pp. 275–284 in: *Clays Controlling the Environment. Proceedings of the 10th International Clay Conference.* (G.J. Churchman, R.W. Fitzpatrick and R.A. Eggleton, editors). CSIRO Publishing, Melbourne, Australia.
Romero, R., Robert, M., Elsass, F., and Garcia, C. (1992) Evidence by transmission electron microscopy of weathering microsystems in soils developed from crystalline rocks. *Clay Minerals*, **27**, 21–33.
Salins, I. and Ringroase-Vose, A.J. (1994) Impregnating techniques for soils and clay materials – the problems and overcoming them. *Technical Report 6/1994.* CSIRO Division of Soils, Canberra.
Sand, L.B. (1956) On the genesis of residual kaolins. *American Mineralogist*, **41**, 28–40.
Senkayi, A.L., Dixon, J.B., Hossner, L.R., Abdur-Rahman, M., and Fanning, D.S. (1984) Mineralogy and genetic relationships of tonstein, bentonite, and lignitic strata in the Eocene Yegua Formation of East-Central Texas. *Clays and Clay Minerals*, **32**, 259–271.
Singh, B. (1996) Why does halloysite roll? – a new model. *Clays and Clay Minerals*, **44**, 191–196.

(*Received 12 July 2009; revised 12 November 2009; Ms. 336; A.E. W.D. Huff*)